Supporting Information

Fyfe et al. 10.1073/pnas.1202593109

SI Text

Materials and Methods. ***Sample preparation and crystallization.*** The thiol-dependent reductase I (*TDR1*) gene (1) from *Leishmania infantum* (LinJ.33.0260, the encoded protein sequence is identical to that of *Leishmania donovani*) was cloned into pET15bTEV to add a tobacco etch virus (TEV) protease cleavable histidine tag as an aid for purification of the recombinant protein. A selenomethionine (SeMet) derivative was prepared in the methionine auxotroph *Escherichia coli* strain B834 (DE3), using selenomethionine medium (Molecular Dimensions), supplemented with 40 mg mL^{-1} SeMet. A purification protocol commonly used in our laboratory was applied (2). In summary, the first stage involved nickel affinity chromatography with a 5 mL Ni-NTA (nitriloacetic acid) column (Qiagen). A linear concentration gradient was applied to elute the product, which was then incubated for 2 h with His-tagged TEV protease at 30 °C, before dialysis at room temperature against 20 mM Tris-HCl (pH 7.8), 150 mM for 1 h. The resulting mixture was applied to the Ni-NTA column, which bound the cleaved His-tag, the protease, and uncleaved TDR1. The TDR1, from which the His-tag had been cleaved, was in the flow-through. Fractions were analyzed using sodium dodecyl sulfate polyacrylamide gel electrophoresis (SDS-PAGE) and those containing TDR1 were pooled. The protein was further purified by size exclusion chromatography using a calibrated Superdex 200 26/60 column (GE Healthcare) equilibrated with 20 mM Tris-HCl, 150 mM NaCl (pH 7.8). This final purification stage also indicated that TDR1 formed a stable trimer in solution. The high level of TDR1 purity was confirmed by SDS-PAGE and matrix-assisted laser desorption/ionization-time-of-flight mass spectrometry. The latter technique also confirmed full incorporation of SeMet. The sample was dialyzed into 10 mM Hepes (pH 7.8), 50 mM NaCl then concentrated using a Vivaspin 20 (Sartorius) to provide a stock solution for crystallization. A theoretical extinction coefficient of 56,185 M^{-1} cm^{-1} at 280 nm, was used to estimate protein concentration (*PROTPARAM*) (3) the theoretical mass of one subunit of the SeMet derivative is 50,872 Da.

TDR1 was crystallized at 20 °C by the hanging drop vapor diffusion method using 0.75 μL of protein solution at a concentration of 5 mg mL^{-1} containing 1 mM glutathione, mixed with 0.75 μL of reservoir containing 12% polyethylene glycol (PEG) 8000, 0.1 M Hepes buffer (pH 7.0), 8% (vol/vol) ethylene glycol. Monoclinic rods, with approximate dimensions of $1.0 \times 0.2 \times 0.2$ mm, grew over 1–2 d. The concentration of PEG 8000 and ethylene glycol in the mother liquor provided sufficient cryoprotection that crystals could be placed in a stream of cold N_2 gas directly and characterized in-house using a Rigaku HF007 rotating anode X-ray generator coupled to an RAXIS IV^{++} image plate detector. The crystals were monoclinic, space group $C2$ with unit cell lengths $a = 197.5$, $b = 58.4$, $c = 160.4$ Å with $\beta = 111.8°$. Crystals were stored in liquid N_2 for data collection at a synchrotron. Attempts to obtain crystals of the apo-form, and of complexes with glutathionylspermidine or trypanothione were unsuccessful.

X-ray data collection, processing, structure solution, and refinement. Single-wavelength anomalous diffraction (SAD) data were measured from a SeMet derivative on beam line I02 of the Diamond Light Source using an ADSC Q315 CCD detector. Data were indexed and integrated using MOSFLM (4) and scaled using SCALA (5). The SAD data were collected near the Se K-absorption edge *f*" maximum, determined using X-ray absorption near edge structure spectroscopy. Initial phases were obtained by SAD-phasing within the Collaborative Computing Project Number 4 pipeline CRANK (6–9). Substructure detection and refinement were performed using AFRO, CRUNCH2 (10), and BP3 (8), and identified the positions of all 39 selenium atoms present. The initial figure-of-merit was 0.49. Hand determination followed by density modification was performed using SOLOMON (11) with an estimated solvent content of 55%, and this improved the figure-of-merit to 0.71. Automated map interpretation with BUCCANEER (12) produced a partial model consisting of 1,335 residues in 15 polypeptide chains giving R_{work} and R_{free} values of 33.5% and 36.9%, respectively. The model was then extended in COOT (13).

Refinement was performed in REFMAC5 (14) utilizing translation/libration/screw refinement (15) and alternated with rounds of electron and difference density map inspection and model manipulation together with ligand incorporation using COOT. Noncrystallographic symmetry restraints were not employed. MOLPROBITY (16) was used to investigate model geometry in combination with the validation tools provided in COOT. Crystallographic statistics are presented in Table 1. Analyses of surface areas and interactions were made using the PISA server (17) and figures were prepared with PyMOL (18). Amino acid sequence alignments were carried out using the program MUSCLE (19) and structural superimposition performed with SSM (20). The PDBeFold server (http://www.ebi.ac.uk/msd-srv/ssm) was used to perform a search of the protein structural database.

Enzyme preparation. TDR1 was expressed and purified using similar protocols to those described above. Trypanothione reductase (TR) was produced in *E. coli* from a pET28a+ construct containing the *L. donovani* trypanothione reductase gene obtained from Prof. Sylke Müller. LinJ27_0760, the gene encoding the *L. infantum* glutaredoxin 1 (*Li*GRX1) and LinJ29_V3.1250, that encoding the cytosolic tryparedoxin type 1 (*Li*TXN1), were cloned into pET15bTEV and the His-tagged proteins purified as described above. Glutathione reductase (GR) from *Saccharomyces cerevisiae* was purchased from Sigma.

Enzyme assays. Thioltransferase, $T(SH)_2$: GSSG (glutathione reductase). The ability of TDR1 and *Li*GRX1 to catalyze reduction of GSSG by trypanothione was assayed in 200 μL of 100 mM Tris-HCl, 5 mM EDTA (pH 7.0), containing 400 μM NADPH, 200 μM GSSG, 200 μM $T(SH)_2$, 1 u mL^{-1} TR. The $T(SH)_2$ was immediately converted to $T(SH)_2$ by TR, leaving an NADPH concentration of 200 μM. The rate of reduction of GSSG by $T(SH)_2$ was then determined by measuring absorbance at 340 nm for 3 min. The thioltransferase reaction was started by addition of 0.3 μM TDR1 or 0.8 μM GRX1 and the A_{340} measured for a further 5 min. The K_m for $T(SH)_2$ was determined with a fixed concentration of GSSG (200 μM) and six different concentrations of $T(SH)_2$ (10–200 μM).

Thioltransferase, reduced glutathione (GSH): $T(S)_2$ (trypanothione reductase). TDR1-enhanced reduction of trypanathione by glutathione reduced form GSH was assayed in 200 μL of 100 mM Tris-HCl, 5 mM EDTA, (pH 7.0) containing 200 μM NADPH, 200 μM GSH, 200 μM $T(S)_2$, 1 u mL^{-1} GR. The spontaneous rate of reduction of $T(S)_2$ by GSH was determined by measuring absorbance at 340 nm for 3 min. The thioltransferase reaction was started by addition of 0.6 μM TDR1 or 2.4 μM *Li*GRX1.

Thioltransferase GSH: 2-ME-SG (hydroxyethyl disulfide (HEDS) assay). 2-ME-SG, the mixed disulfide of GSH and β-mercaptoethanol, is formed during a 3 min preincubation of GSH and HEDS. The assay, a standard for glutaredoxin (21–24), measures deglutathionylation of the mixed disulfide. One milliliter of 50 mM Tris-HCl, 5 mM EDTA (pH 7.0), containing 200 μM NADPH, 750 μM HEDS, 1 mM GSH, and 1 u mL^{-1} GR was incubated for 3 min at 30 °C. The thioltransferase reaction was started by addition of 20 nM TDR1 or 60 nM *Li*GRX1 and the rate was determined by measuring A_{340} for 5 min. The K_m for 2-ME-SG was determined with a fixed concentration of GSH (1 mM) and six different concentrations of $T(S)_2$ (0.1–2.0 mM).

Thioltransferase $T(SH)_2$: 2-ME-SG (HEDS assay). Reactions were carried out in 200 μL of 50 mM Tris-HCl, 5 mM EDTA containing 400 μM NADPH, 750 μM HEDS, 200 μM $T(S)_2$, 1 u mL^{-1} TR, 6 μM TDR1. In this reaction the $T(S)_2$ is immediately reduced to $T(SH)_2$ by TR, leaving 200 μM NADPH. Reactions were started by adding TDR1 without preincubation of $T(SH)_2$ and HEDS. This is because a high spontaneous rate of reduction was observed for the mixed disulfide formed between $T(SH)_2$ and β-mercaptoethanol.

Peroxidase.

With GSH and hydrogen peroxide.
Reactions were carried out in 1 mL of 50 mM Tris-HCl, 5 mM EDTA (pH 7.0), containing 200 μM NADPH, 1 μM GSH, 1 u mL^{-1} GR, 20 μM or 250 μM H_2O_2, and 0.6 μM TDR1 or 1.7 μM *Li*GRX1. Reactions were started by addition of the dithiol protein and the rate was determined by measuring the absorbance at 340 nM for 5 min.

With GSH and organic hydroperoxide.
Reactions were carried out in 1 mL of 50 mM Tris-HCl, 5 mM EDTA (pH 7.0), containing 200 μM NADPH, 1 mM GSH, 1 u mL^{-1} GR, 250 μM cumene hydroperoxide or 250 μM tert-butyl hydroperoxide, and 2.4 μM TDR1 or 9 μM *Li*GRX1. Reactions were started by addition of the enzyme and the rate was determined by measuring the absorbance at 340 nM for 5 min.

Protein disulfide reductase (insulin reductase).

With trypanothione as the reducing agent.
Reactions carried out in 200 μL 50 mM Tris-HCl, 5 mM EDTA (pH 7.0), containing 400 μM NADPH, 200 μM $T(S)_2$, 1 u mL^{-1} TR, 300 μg mL^{-1} bovine insulin, and 6 μM TDR1 or 5 μM *Li*GRX1 or 6 μM tryparedoxin 1 (*Li*TXN1). Reactions were set up without the dithiol protein and the absorbance at 340 nm indicated that the concentration of NADPH was immediately reduced from 400 μM to 200 μM following complete reduction of $T(S)_2$. Reactions were started by adding the dithiol protein and the rates determined by measuring the absorbance at 340 nm for 5 min.

With GSH as the reducing agent.
Reactions carried out in 200 μL 50 mM Tris-HCl, 5 mM EDTA (pH 7.0), containing 200 μM NADPH, 1 mM GSH, 1 u mL^{-1} GR, 300 μg ml^{-1} bovine insulin, and 6 μM TDR1 or 5 μM *Li*GRX1 or 6 μM *Li*TXN1. Reactions were started by adding the dithiol containing protein and the rate determined by measuring the absorbance at 340 nm for 5 min. To determine whether TDR1 could act as a reducing agent for *Li*TXN1 in this system, TDR1 was added to a reaction containing *Li*TXN1.

Deglutathionylation with a glutathionylated peptide as a substrate. 200 μL of 50 mM Tris-HCl pH 7.0, 5 mM EDTA (pH 7.0), containing 125 μM NADPH, 1 u mL^{-1} GR, 250 μM GSH, and 100 nM TDR1 or 50 nM *Li*GRX1 was incubated for 5 min at 30 °C before starting the reaction by addition of 100 μM of the glutathionylated peptide (peptide-SG).

1. Denton H, McGregor JC, Coombs GH (2004) Reduction of anti-leishmanial pentavalent animonial drugs by a parasite-specific thiol-dependant reductase, TDR1. *Biochem J* 381:405–412.
2. Dawson A, Fyfe PK, Hunter WN (2008) Specificity and reactivity in menaquinone biosynthesis; the structure of *Escherichia coli* MenD [2-succinyl-5-enolpyruvyl-6-hydroxy-3-cyclohexadiene-1-carboxylate synthase]. *J Mol Biol* 384:1353–1368.
3. Gasteiger E, et al. (2005) . Protein identification and analysis tools on the ExPASy server. The proteomics protocols handbook, Humana Press, New York, 571–607.
4. Leslie AGW (2006) The integration of macromolecular diffraction data. *Acta Cryst D*62:48–57.
5. Evans P (2006) Scaling and assessment of data quality. *Acta. Cryst* D62:72–82.
6. Ness SR, de Graff AG, Abrahams JP, Pannu NS (2004) CRANK: New methods for automated macromolecular crystal structure solution. *Structure* 12:1753–1761.
7. Pannu NS, Read RJ (2004) The application of multivariate statistical techniques improves single-wavelength anomalous diffraction phasing. *Acta Cryst* D60:22–27.
8. Pannu NS, McCoy AJ, Read RJ (2003) Application of the complex multivariate normal distribution to crystallographic methods with insights into multiple isomorphous replacement phasing. *Acta Cryst* D59:1801–1808.
9. Pannu NS et al. (2011) Recent advances in the CRANK software suite for experimental phasing. *Acta Cryst* D67:331–337.
10. de Graaf RAG, Hilge M, van der Plas JL, Abrahams JP (2001) Matrix methods for solving protein substructures of chlorine and sulfur from anomalous data. *Acta Cryst* D57:1857–1862.
11. Abrahams JP, Leslie AGW (1996) Methods used in the structure determination of bovine mitochondrial F1 ATPase. *Acta Cryst* D52:30–42.
12. Cowtan K (2006) The Buccaneer software for automated model building *Acta Cryst*. D62:1002–1011.
13. Emsley P, Cowtan K (2004) Coot: Model building tools for molecular graphics. *Acta Cryst* D60:2126–2132.
14. Murshudov GN, Vagin AA, Dodson EJ (1997) Refinement of macromolecular structures by the maximum-likelihood method. *Acta Cryst* D53:240–255.
15. Winn M, Isupov M, Murshudov GN (2000) Use of TLS parameters to model anisotropic displacements in macromolecular refinement. *Acta Cryst*D57:122–133.
16. Chen VB et al. (2010) MolProbity: All-atom structure validation for macromolecular crystallography. *Acta Cryst* D66:12–21.
17. Krissinel E, Henrick K (2007) Inference of macromolecular assemblies from crystalline state. *J Mol Biol* 372:774–797.
18. DeLano WL (2002) The PyMOL Molecular Graphics System, http://www.pymol.org.
19. Edgar RC (2004) MUSCLE: Multiple sequence alignment with high accuracy and high throughput. *Nucleics Acid Res* 32:1792–1797.
20. Krissinel E, Henrick K (2004) Secondary-structure matching (SSM), a new tool for fast protein structure alignment in three dimensions. *Acta Cryst* D60:2256–2268.
21. Axarli I, Dhavala P, Papageorgiou AC, Labrou NE (2009) Crystal structure of *Glycine max* glutathione transferase in complex with glutathione: Investigation of the mechanism operating by the Tau class glutathione transferases. *Biochem J* 422:247–256.
22. Cheng G, Ikeda Y, Iuchi Y, Fujii J (2005) Detection of S-glutathionylated proteins by glutathione S-transferase overlay. *Arch Biochem Biophys* 435:42–49.
23. Peltoniemi MJ, Karala AR, Jurvansuu JK, Kinnula VL, Ruddock LW (2006) Insights into deglutathionylation reactions. Different intermediates in the glutaredoxin and protein disulfide isomerase catalyzed reactions are defined by the gamma-linkage present in glutathione.*J Biol Chem* 281:33107–33114.
24. Johansson C, Lillig CH, Holmgren A (2004) Human mitochondrial glutaredoxin reduces S-glutathionylated proteins with high affinity accepting electrons from either glutathione or thioredoxin reductase. *J Biol Chem* 279:7537–7543.

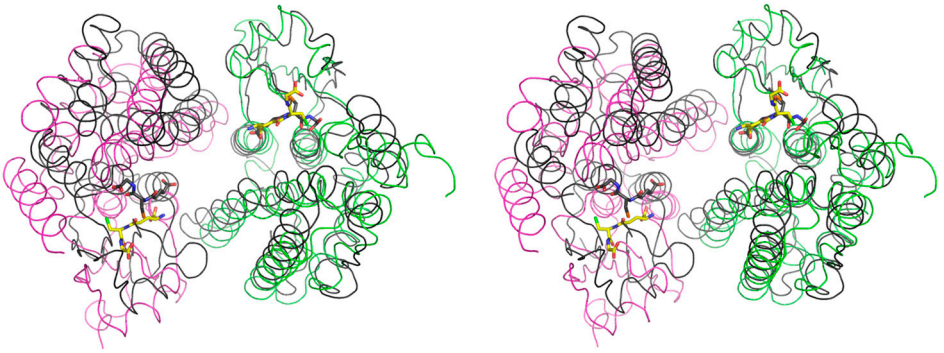

Fig. S1. Stereoview comparison of TDR1 intersubunit (*A*–*C*) dimer with the dimer formed by the closest structurally related tau class GST dimer [PDB code: 3FHS(21)]. The polypeptide trace of 3FHS is shown in dark gray, superimposed on domain I from subunit A (green) and domain II from subunit C (purple), which generate the TDR1 GST-like dimer. The bound glutathione molecules are depicted as sticks colored yellow for C in the TDR1 model, gray in the 3FHS model.

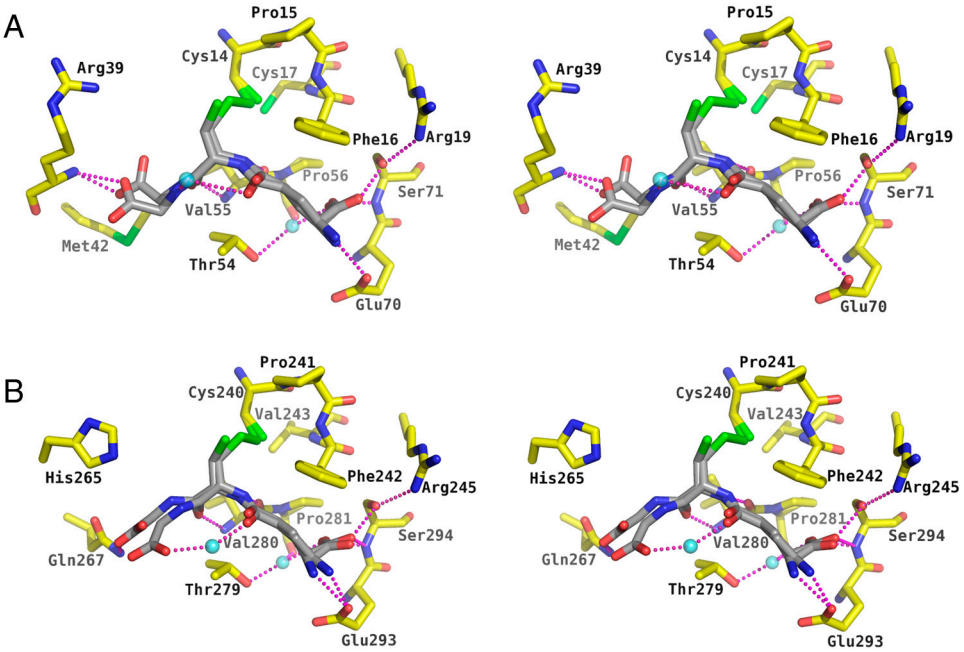

Fig. S2. Stereoview images of the glutathione binding sites within subunit A. (*A*) G-Ithe domain I glutathione binding site. (*B*) G-II—the domain II binding site. Atomic positions are color coded: N blue, O red, S green, C gray for the ligands and yellow for the protein. Water molecules are shown as cyan spheres. Dotted lines represent potential hydrogen bonding interactions. Glutathione is present as a mixture of reduced and oxidized forms.

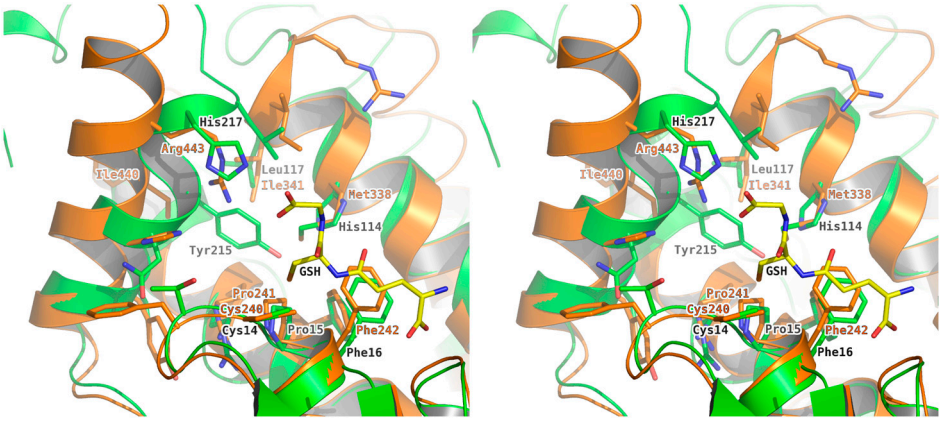

Fig. S3. Stereo image showing an overlay of the hydrophobic (H-sites) from domain I (H-I, green) and domain II (H-II, orange) from subunit A. The Cys-Pro-Phe motif is conserved in both sites. The H-I pocket is restricted by the positioning of Tyr215 and His114 together with the placement of α12.

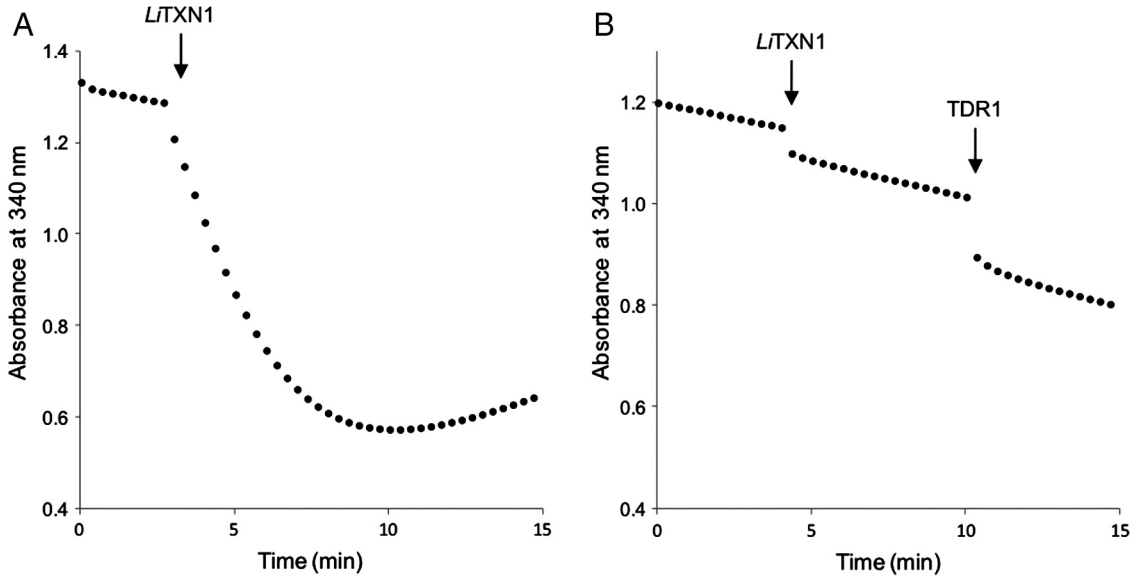

Fig. S4. TDR1 is unable to act as a reducing agent for tryparedoxin (*Li*TXN1) in the reduction of bovine insulin. (*A*) Disulphide reductase activity of tryparedoxin (*Li*TXN1) with a trypanothione reducing system. The initial reaction contains 200 μM trypanothione, 1 u/mL trypanothione reductase, 200 μM NADPH, and 300 μg/mL bovine insulin. *Li*TXN1 was added at the time indicated to give a final concentration of 6 μM, completing a redox couple in which NADPH, TR, and $T(SH)_2$ act as reductants for *Li*TXN1 and insulin is the final electron acceptor. In this reaction, insulin reduction is coupled to NADPH oxidation, which is detected by measuring the absorbance at 340 nm. (*B*) LITXN1 is unable to use glutathione or TDR1 as a reductant. The initial reaction contains 1 mM glutathione, 1 u/mL glutathione reductase, 200 μM NADPH, and 300 μg/mL bovine insulin. *Li*TXN1 does not bind glutathione and is unable to use a glutathione reducing system, so there was no increase in the consumption of NADPH when the protein (10 μM final concentration) was added to the reaction. Addition of TDR1 to a final concentration of 15 μM had no effect on the rate of NADPH oxidation, indicating that TDR1, which uses the glutathione reducing system, was not able to complete the redox couple by acting as a reductant for *Li*TXN1.

Table S1. Crystallographic statistics

Data collection	
Space group	*C*2
Wavelength	0.9795 Å
Unit cell parameters	
a, *b*, *c*, (Å)	197.5, 58.4, 160.4
β (°)	111.8
Resolution range (Å)	29.8–2.3
Unique reflections	74,464
Completeness (%)*	97.9 (98.7)
$\langle I/\sigma(I)\rangle$	12.6 (3.9)
Multiplicity	4.0 (4.2)
R_{merge} (%)†	5.9 (25.9)
Refinement	
Resolution range (Å)	30.0–2.3
No. of used reflections	70,625
R_{work}‡, R_{free}§	14.9, 20.8
Protein atoms	11,011
Glutathione/ethylene glycol/water	6, 15, 1,165
Rms deviations from ideal geometry	
bond lengths (Å)	0.015
bond angles (°)	1.418
Thermal parameters (Å^2)	
Wilson *B*	42.9
Mean *B* Subunit A, B, C	55.2/60.5/55.9
GSH, water, ethylene glycol	46.8/60.2/72.7
Ramachandran plot (%) favored/allowed	98.3/1.2/0.5

*Values in parentheses refer to the highest resolution bin of width approx. 0.1 Å.

†$R_{merge} = \sum h \sum i|(h, i)\text{-}\langle I(h)\rangle| \sum h \sum i I(h, i)$.

‡$R_{work} = \sum hkl||F_o|\text{-}|F_c||/\sum |F_o|$, where F_o is the observed structure factor and F_c the calculated structure factor.

§R_{free} is the same as R_{work} except calculated using 5% of the data that are not included in any refinement calculations.

Table S2. Kinetic parameters of peptide deglutathionylation catalyzed by TDR1 and different glutaredoxins (GRXs)

Species	Enzyme	Substrate	K_m μM	k_{cat} s^{-1}	k_{cat}/K_m M^{-1} s^{-1}	Reference
L. infantum	TDR1	peptide-SG	433	6.5	1.5E+04	23
L. infantum	GRX1	peptide-SG	7.6	1.0	1.30E+05	23
E. coli	GRX1	peptide-SG	7.8	4.4	5.13E+05	24
E. coli	GRX1(C14S)	peptide-SG	44	4.0	9.09E+04	24
Human	GRX1	RNase-SG	4.1	6.8	1.70E+06	25
Human	GRX2	RNase-SG	0.8	1.9	2.50E−06	25
T. brucei	GRX1	TXNPx-SG	21	1.5	6.90E+04	26
T. brucei	GRX2	TXNPx-SG	269	1.0	3.80E+03	26

Results for TDR1 and *Li*GRX1 are the means of two independent experiments. Enzymes: *E. coli* GRX1 (C14S) is an active site mutant of the GRX1; *E. coli* GRX1 is the homolog of *Li*GRX1. *Tb*GRX2 has the active site motif CQFC and only 25% amino acid identity with *Tb*GRX1 (1). The *Leishmania* homolog of GRX2 has only one cysteine in the active site (CQFS). Substrates: peptide-SG, SQLWCLSN with GSH linked to the cysteine by a disulfide bond; RNase-SG, glutathionylated ribonuclease A: TXNPx-SG, glutathionylated tryparedoxin-dependent peroxidase.

1 Ceylan S et al. (2010) The dithiol glutaredoxins of African trypanosomes have distinct roles and are closely linked to the unique trypanothione metabolism. *J Biol Chem* 285:35224–35237.